AIAA JOURNAL
Vol. 32, No. 4, April 1994

# Dynamic Pitch-Up of a Delta Wing

O. K. Rediniotis,* S. M. Klute,* N. T. Hoang,* and D. P. Telionis†
*Virginia Polytechnic Institute and State University, Blacksburg, Virginia 24061*

**The transient flowfield over a delta wing during pitch-up motions to very large angles of attack was investigated. Emphasis was directed at the growth and the eventual breakdown of the leading-edge vortices. Delta wing models were tested in a wind tunnel at Reynolds numbers of order $10^5$. The flowfield along the trailing edge was mapped out via a seven-hole probe designed, constructed, and calibrated to generate time-resolved information. Instantaneous surface pressure measurements were also obtained. Earlier qualitative evidence of hysteresis in the development of the flow was confirmed. Moreover, the present data indicate significant differences of vorticity content between the steady and the unsteady motions, for reduced frequencies as low as 0.01.**

## Nomenclature

| | | |
|---|---|---|
| $C$ | = | chord length |
| $C_p$ | = | pressure coefficient |
| $h$ | = | wing thickness |
| $k_{ave}$ | = | average nondimensional pitch rate, $\dot{\alpha}_{ave}C/2U$ |
| $L$ | = | leading-edge length (see Fig. 1) |
| $L'$ | = | model length from apex to trailing edge, measured along axis $x'$ (see Fig. 1) |
| $r$ | = | radial distance from vortex core |
| $S_0$ | = | wing's half-span (measured along the trailing edge) |
| $S(x)$ | = | local half-span measured at location $x$, along $y$ axis |
| $U$ | = | freestream velocity |
| $X, Y, Z$ | = | coordinate system aligned with measurement plane A (see Fig. 3) |
| $X', Y', Z'$ | = | coordinate system aligned with measurement plane B (see Fig. 3) |
| $x, y, z$ | = | coordinate system aligned with the wing's leading edge (see Fig. 1) |
| $x'$ | = | coordinate axis along the axial pressure port line (see Fig. 1) |
| $\alpha$ | = | angle of attack |
| $\dot{\alpha}_{ave}$ | = | average pitch rate |
| $\Lambda$ | = | sweep angle |
| $\Omega$ | = | nondimensional vorticity |

## I. Introduction

ONBOARD computers and modern technologies in propulsion and materials will allow combat aircraft to operate over a much expanded maneuvering envelope. These technologies have outpaced our understanding of unsteady aerodynamics. Some of the desirable maneuvers will require a swift pitch-up motion and/or a roll about the velocity vector at high angles of attack. A good model for the study of unsteady aerodynamics at high angles of attack is the delta wing. The dynamics of a pitching delta wing were considered as early as 1969.[1] However, the bulk of the contributions on this topic appeared only in the past few years.[2-15] The practical aspects of possible aircraft maneuvers are discussed in Refs. 16-18. Nguyen and Gilbert[18] provide a discussion on the impact of emerging technologies on the potential of the next generation of combat aircraft. In the present paper we confine our attention to the aerodynamics of a delta wing in a sharp, ramp-like pitch-up motion.

The flow over a delta wing at a fixed angle of attack is dominated by two leading-edge vortices. The circumferential velocity component along a plane normal to such a vortex is reminiscent of a potential vortex with a viscous core, whereas the axial component resembles a jet. The structure is symmetric about the symmetry plane of the wing. Compared to two-dimensional airfoils, lift stall is greatly delayed to angles of attack as large as 30 deg. A large number of researchers have studied this steady flow problem, and many reviews have appeared.[19] Recent investigators reported on the use of powerful experimental techniques, like laser-Doppler velocimetry (LDV), double cross wires, or particle image velocimetry, and documented quantitatively the complex vortical fields over delta wings.[20-25]

A phenomenon that cannot be avoided in all three-dimensional flows over bodies at large angles of attack is vortex breakdown. Several investigations of the leading-edge vortex breakdown have appeared.[26-29] The imprint of a vortex, namely, the pressure distribution on the solid surface, clearly displays the basic characteristics of this phenomenon. The suction peak of a well-organized vortex disappears. If the pressure is observed along a ray and the increasing parameter is the angle of attack, then again bursting can be identified as a sudden drop of suction peak pressure.[29]

In the steady-flow case, the predominant direction of convection is the direction of the mean flow. The vortex is fed with vorticity all along the length of the leading edge. It appears then physically reasonable and, in fact, it has been demonstrated analytically[30] and experimentally[31] that in some cases, the flow is very nearly conical. The physics of the problem change drastically if the angle of attack is increased dynamically. For rapid pitch-up motions leading to large angles of attack, events are influenced mostly by local phenomena. The dominant direction of convection changes. This aspect of the flow is bound to influence both the development of the vortex as well as its breakdown characteristics.

The past three years have seen a lot of activity in the area of unsteady aerodynamics of delta wings. A more complete list with the basic parameters of most of the experimental efforts in this area can be found in Table 1.1 of Ref. 32. Most studies indicate great departures from the quasisteady field, which often manifests themselves in the form of hysteresis loops, if periodic motions are employed. With the exception of the work of Thompson et al.[13] and Magness et al.,[14,15] these research programs aim mostly at global characteristics like lift

Received Dec. 24, 1992; revision received Aug. 2, 1993; accepted for publication Sept. 24, 1993. 

*Graduate Research Assistant, Department of Engineering Science and Mechanics.

†Professor, Department of Engineering Science and Mechanics. Associate Fellow AIAA.

or drag. When the dynamic behavior of the flowfield is studied, this is done almost exclusively through flow visualization. Very little effort has been directed in documenting quantitatively the detailed structure of the flow. The team of Refs. 14 and 15 is the only one reporting on unsteady, two-component velocity measurements using particle image velocimetry (PIV). The PIV method captures an instantaneous snapshot of an entire plane of a velocity field. On the other hand, to measure the unsteady velocity field with LDV, one must use ensemble averaging and obtain data through many cycles of motion displacing the measuring volume from point to point. Magness et al.[14,15] employed the PIV method to measure velocity components along one plane normal to the vortex. Their data were obtained during pitch-up and pitch-down motions but only at the instant that the angle of attack is equal to 45 deg. The history of the vortical development has not yet been quantitatively documented. Moreover, with only two of the components of the velocity obtained, only the axial vorticity component could be calculated. Pressure measurements on the suction surface of a delta wing were obtained for a pitching wing. However, the reduced frequency of pitching was rather high (0.1–0.3) and, therefore, the flow was locked onto a periodic motion. Moreover, the angles of attack ranged between 30 and 40 deg which is rather low for comparison with the data presented here.

In this paper we present measured data on the developing velocity and vorticity fields, during pitch-up motions. Three components of both quantities, velocity and vorticity, are documented, and the complete history of these fields is recorded along two planes up to angles of attack as large as 68 deg. Unlike all earlier data, the present results present the development of the flowfield during the pitch-up motion. A comprehensive review on such issues can be found in Ref. 33. These data are complemented with instantaneous pressure distributions on the suction surface of the model. Issues, like vortex breakdown behavior, its time lag with respect to the steady case, and the effect of this lag on the pressure field, are discussed. The vorticity content (axial and lateral components) of the dynamically evolving leading-edge vortex and its interaction with the trailing-edge shed vorticity are investigated.

## II. Facilities, Models, and Instrumentation

Tests were conducted in the Engineering Science and Mechanics (ESM) wind tunnel. This wind tunnel has a 0.508-m × 0.508-m test section and is equipped with a mechanism that can perform dynamic motions of the model. The moving frame can swing over a range of 90 deg about a horizontal axis which in turn can be adjusted to pass through any point of the upper half-chord of the model. The driving power is provided by a 3/4-hp dc motor through either a 16:1 or a 5:1 ratio speed reducer, depending on the maximum required pitch rate. The speed of the motor can be varied through a controller which in turn is activated by a laboratory computer. The pitching mechanism is equipped with an optical encoder for angle-of-attack information, as well as a triggering device for phase information and synchronization. The estimated angle of attack accuracy is 0.2 deg. The system can generate arbitrary time schedules of motion.

Two delta wing models with sweep angle $\Lambda = 75$ deg were employed. The first was a solid model with root chord $C = 0.304$ m and thickness $h = 6$ mm. Its leading edges were beveled at 29 deg. The second was instrumented with pressure transducers. This model had a root chord of $C = 0.345$ m, thickness $h = 16$ mm, and its leading edges were beveled at 45 deg. The distribution of the surface pressure ports, on the leeward side of the second model, is shown in Fig. 1. Pressure taps were provided along a ray that runs underneath the estimated location of the leading-edge vortex core as well as along two lines normal to the leading edge. The location of the leading-edge vortex was determined by earlier pressure measurements along normals to the wing leading edge. These

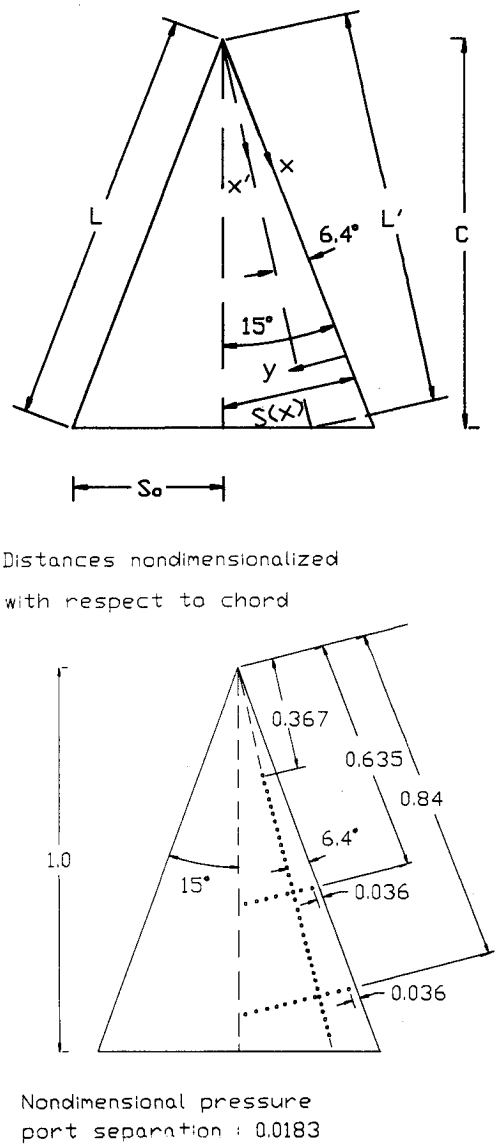


**Fig. 1 Coordinate systems used for the pressure data and pressure port distribution on the leeward side of the model; all dimensions are reduced by the chord length $C$.**

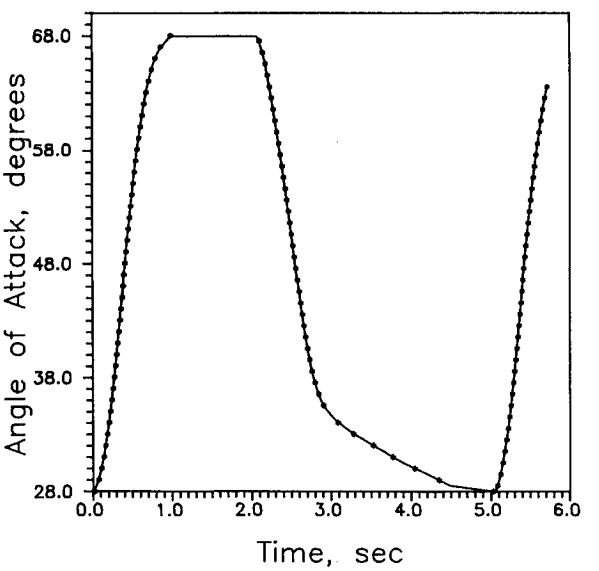


**Fig. 2 Dynamic motion of the model presented as a temporal function of the angle of attack; data were obtained only during pitch-up.**

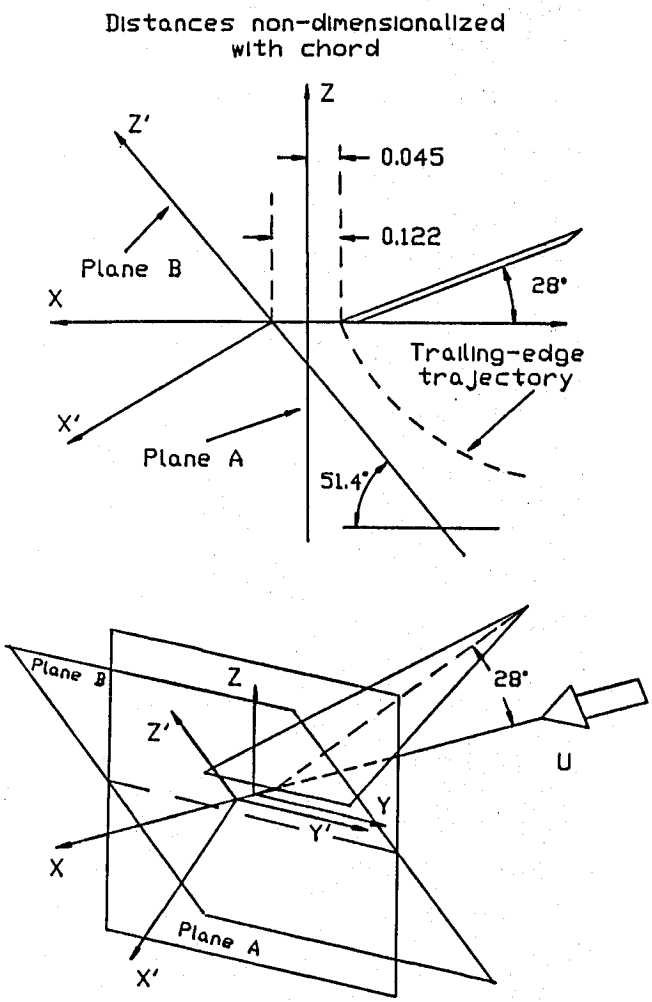


Fig. 3 Definition of coordinate systems for the velocity data, obtained along the fixed planes A and B.

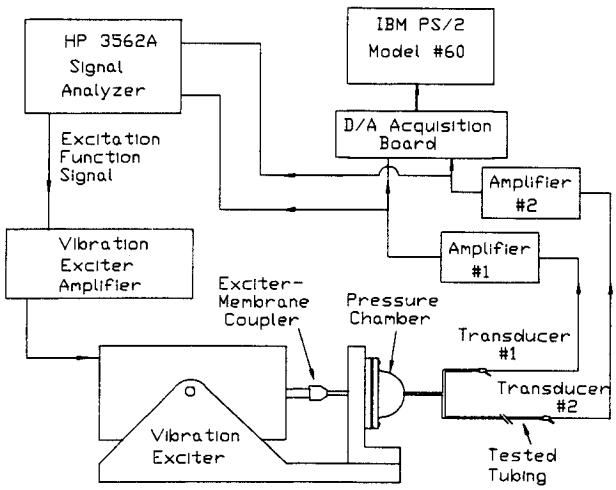


Fig. 4 Seven-hole probe frequency-response measurement setup.

data indicate that there is no significant tendency for the vortex to shift sidewise as the angle of attack increases. The definition of the pressure port coordinate system and the model's characteristic lengths are also shown in this figure.

The models were mounted on the dynamic strut and were pitched about their apex. The schedule employed here involved a rapid increase of the angle of attack as shown in Fig. 2, from an initial value of $\alpha = 28$ deg to a final value of $\alpha = 68$ deg. The angle of attack was kept fixed at the final angle for about 2 s. The average pitch rate was $\dot{\alpha}_{ave} = 0.7$ rad/s. This corresponds to an average nondimensional pitch rate of

$$k_{ave} = \frac{\dot{\alpha}_{ave} C}{2U} = 0.0089$$

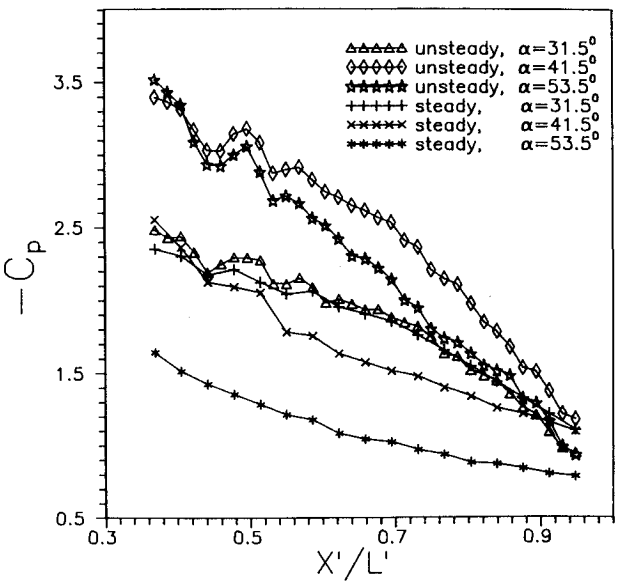


Fig. 5 Pressure distributions for steady and unsteady flow along the axis $x'$; all pressure measurements presented in this figure as well as all subsequent pressure plots have an estimated uncertainty of 2%.

Surface pressures were measured by Endevco transducers mounted on the model. The full scale reading of these transducers was ±100 Torr which corresponds to a ±220-mV transducer output. After a few hours of operation, a drift of about 0.1 mV was observed. To improve on the accuracy of the measurements, we calibrated these instruments before testing. It was thus confirmed that the error was not more than 0.05 mV (or equivalently, 0.023 Torr) at any time during the data taking process.

Velocity data were obtained along two planes as shown in Fig. 3. Plane A was normal to the oncoming stream, positioned downstream of the trailing edge when the wing was at its initial position, namely, at $\alpha = 28$ deg. Plane B was rotated by a fixed angle of 38.6 deg with respect to plane A (Fig. 3) to capture the velocity field closer to the trailing edge during its motion. Both sets of data provide a cross section of the vorticity field shed by the wing and, therefore, contain the accumulated history of events that occurred over the wing surface during its dynamic motion. Velocity data were also conditionally averaged over 25 realizations of the motion.

The velocity field was measured by a seven-hole probe. This probe was designed, constructed, and calibrated especially for this project and is described in detail in Ref. 32. To obtain time-varying data, seven Endevco transducers were connected via short hoses to the seven-hole probe. These hoses were 30 cm long and had an inside diameter of 0.8 mm. The frequency response of this instrument was studied by the setup shown in Fig. 4. A modal exciter, capable of generating frequencies of up to 10 kHz, was employed to drive the membrane of the pressure chamber. The pressure disturbance thus generated, was sensed by two transducers: transducer 1, which was mounted right at the exit of the chamber and transducer 2, communicating with the chamber through a 30-cm-long, 0.8-mm-i.d. hose. The frequency as well as the amplitude of the generated pressure fluctuations could be adjusted. The corresponding transfer function could be calculated by sampling the two transducer outputs. The amplitude and phase characteristics are described in Ref. 32. It was found that for frequencies of the order of 25 Hz the amplitude attenuation is about 1.7% whereas the phase lag is less than 6.5 deg. It

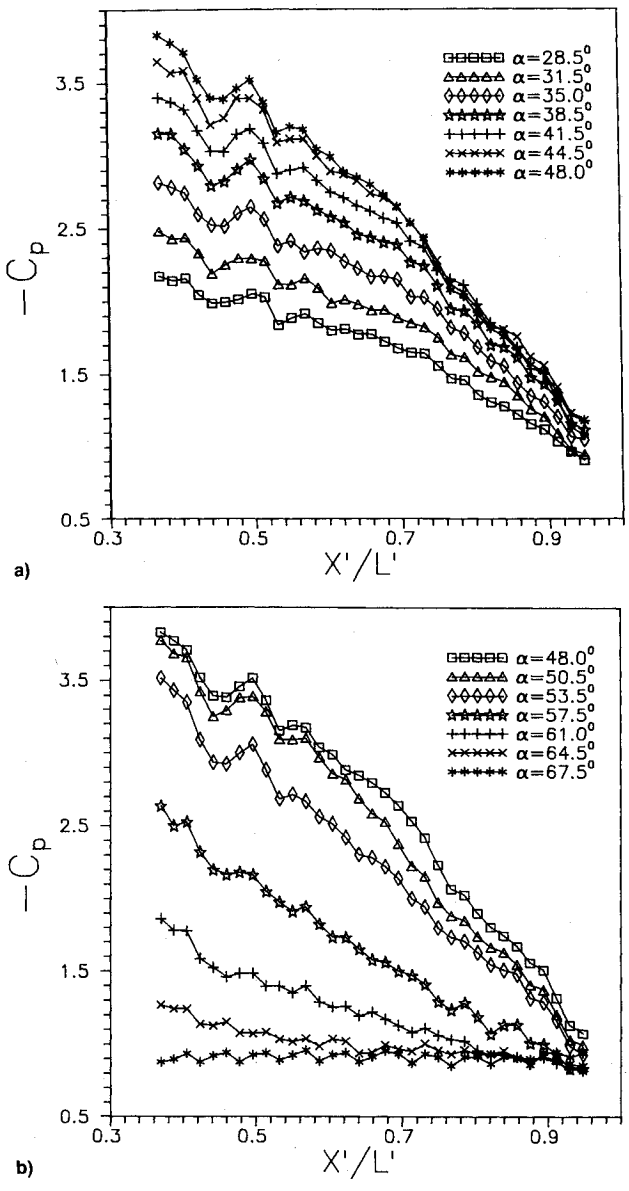


**Fig. 6 Pressure distributions during pitch-up along the axis $x'$: a) $\alpha$ = 28.5 to 48.0 deg and b) $\alpha$ = 48.0 to 67.5 deg.**

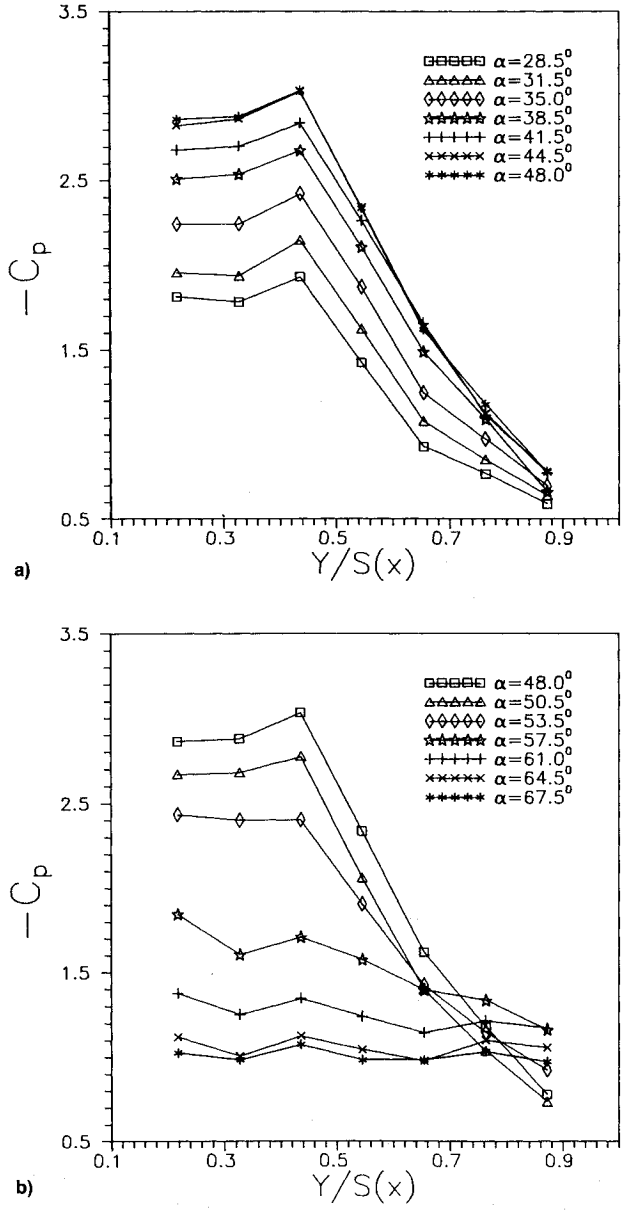


**Fig. 7 Pressure distributions across the vortex at $x'/L'$ = 0.61 during pitch-up: a) $\alpha$ = 28.5 to 48.0 deg and b) $\alpha$ = 48.0 to 67.5 deg.**

should be recalled that the typical time scale of the phenomena under consideration here is about 1 s, whereas the spiral flow instabilities have a time scale about one order of magnitude smaller. Thompson et al.[13] employed connecting tubing about three times as long and made similar observations.

## III. Results and Discussion

Pressure distributions on the suction side of the model are presented first. These are pressures along the axis $x'$ as shown in Fig. 1. For steady flow, all earlier studies indicate that the pressure trough beneath the axis of the vortex has its lowest value near the apex and this value increases toward the trailing edge. This trend is evident in the data presented in Fig. 5. In all of the pressure distributions presented here in terms of the axial distance $x'$, some distortions appear near the apex. This behavior was investigated carefully by changing the pressure transducers employed. It appears to be consistent for all models tested in two different tunnels. It is believed that this behavior is due to the unusual shape of the model near the apex of the wing. The model's cross section very near the apex is triangular and changes over to trapezoidal. For short distances from the apex, the thickness is not much smaller than the span and, therefore, the model is far from a flat plate.

As the angle of attack increases, the pressure over the suction side of the wing decreases, thus generating higher values of lift. However, this is reversed when breakdown sets in. For steady flow, breakdown on a 75-deg-sweep wing moves over the wing at about 32 deg. The steady-flow data in Fig. 5 present indeed a continuous increase of the pressure from $\alpha$ = 31.5 to 42.5 and 54.5 deg. For steady flow, therefore, the suction levels are reduced as the angle of attack increases. However, for the same angles of attack and unsteady flow, the pressure drops continuously.

More detailed pressure distributions for dynamic motions of the model are shown in Fig. 6. Once again, the pressure levels continue dropping for angles of attack far larger than the steady case. Moreover, a very interesting phenomenon can be observed. When eventually the trend is reversed, pressures rise simultaneously at all points. This may indicate that if breakdown occurs, it may not creep up from the trailing edge as it does in the steady case but, instead, it may cover the entire length of the wing within an increase of a few degrees in the angle of attack, as shown in Fig. 6b.

Pressure distributions were also plotted along normals to the leading edge. Figures 7 and 8 present dynamic pressure data along $x'/L'$ = 0.61 and 0.81, respectively. Figure 7 pre-

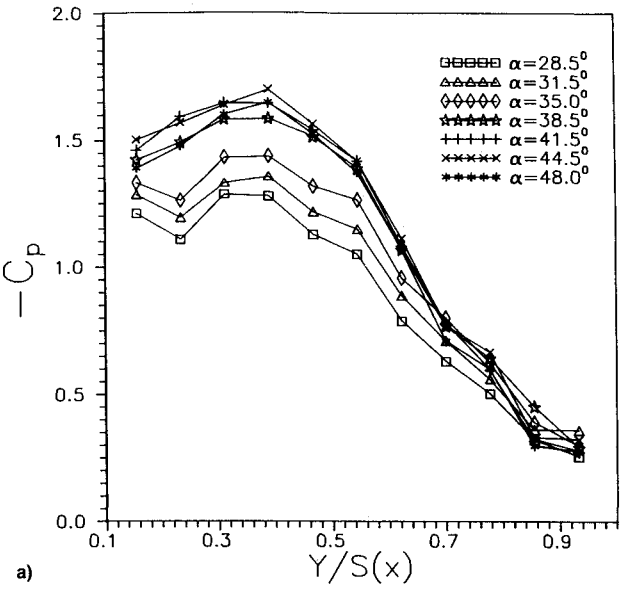


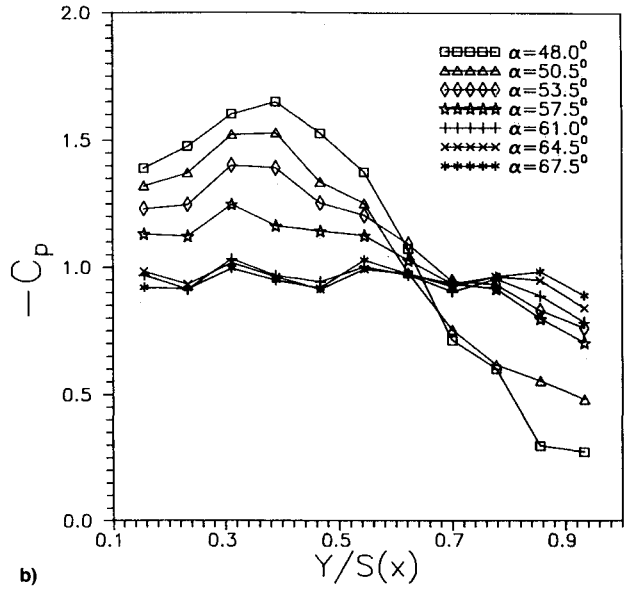


**Fig. 8 Pressure distributions across the vortex at $x'/L' = 0.81$ during pitch-up: a) $\alpha = 28.5$ to 48.0 deg and b) $\alpha = 48.0$ to 67.5 deg.**

sents a comparison of pressure distributions, along $x'/L' = 0.61$, for the dynamic case and the steady case. The behavior discussed earlier is again evident for the cross section of the vortex, namely, the trends for steady and unsteady flow beyond $\alpha = 31.5$ deg are opposite. For steady flow, the suction troughs become more shallow as we increase the angle of attack beyond $\alpha = 31.5$ deg. However, a strong delay is observed again in data obtained during pitch-up, as shown in Figs. 7–9. This is in agreement with earlier flow visualization studies.[33] For unsteady flow, the trough appears to deepen continuously until $\alpha = 46$ deg, and at $x'/L' = 0.61$, a pressure coefficient value of $-3.0$ is achieved, which should be contrasted to the minimum steady-state value of $-2.0$ of Fig. 7.

We observe that the curves at both stations, $x'/L' = 0.61$ and 0.81, reverse their trend at the same angle of attack, namely, between $\alpha = 46$ deg and $\alpha = 48$ deg. This is more evidence indicating that breakdown may occur almost simultaneously along the entire chord of the wing. Moreover, the onset of this phenomenon does not signal a sharp flattening of the pressure profile. Instead, the trough gradually becomes more shallow, indicating that perhaps the core of the vortex breaks down first, and this event spreads smoothly radially outward, all along the length of the vortex.

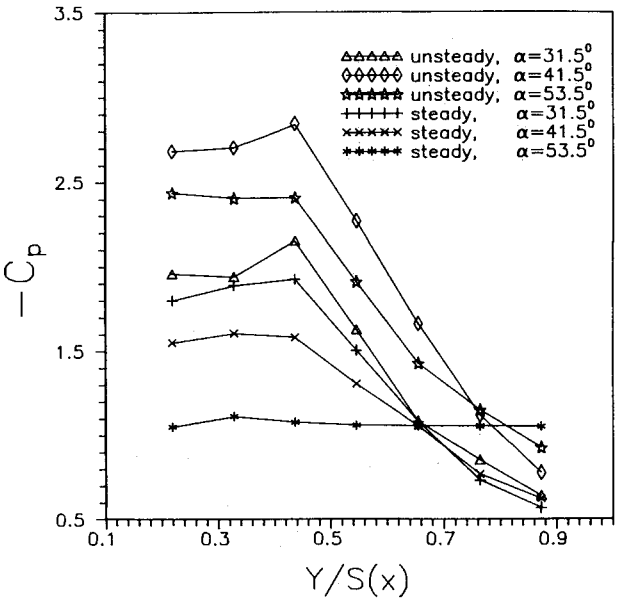


**Fig. 9 Pressure distributions across the vortex at $x'/L' = 0.61$ for steady and unsteady flow.**

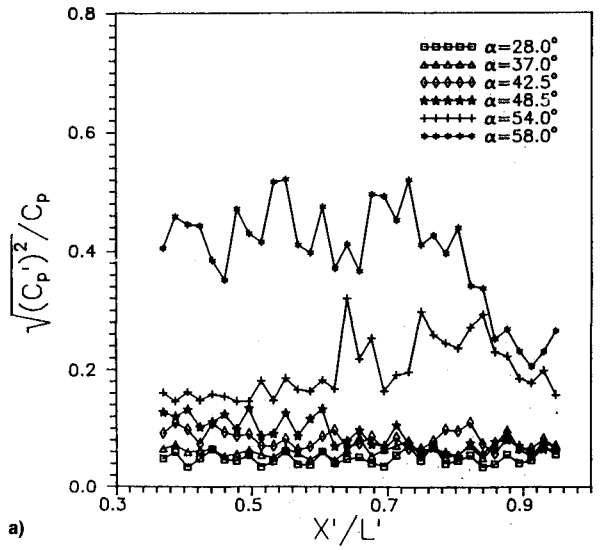


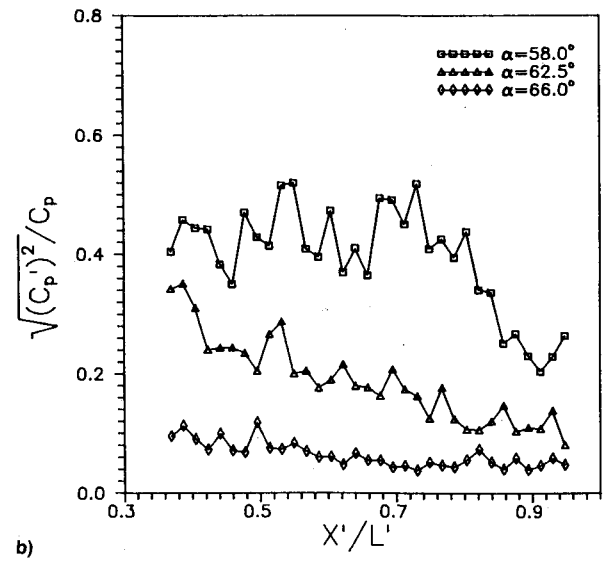


**Fig. 10 Root-mean-square pressure distributions along $x'$ axis during pitch-up.**

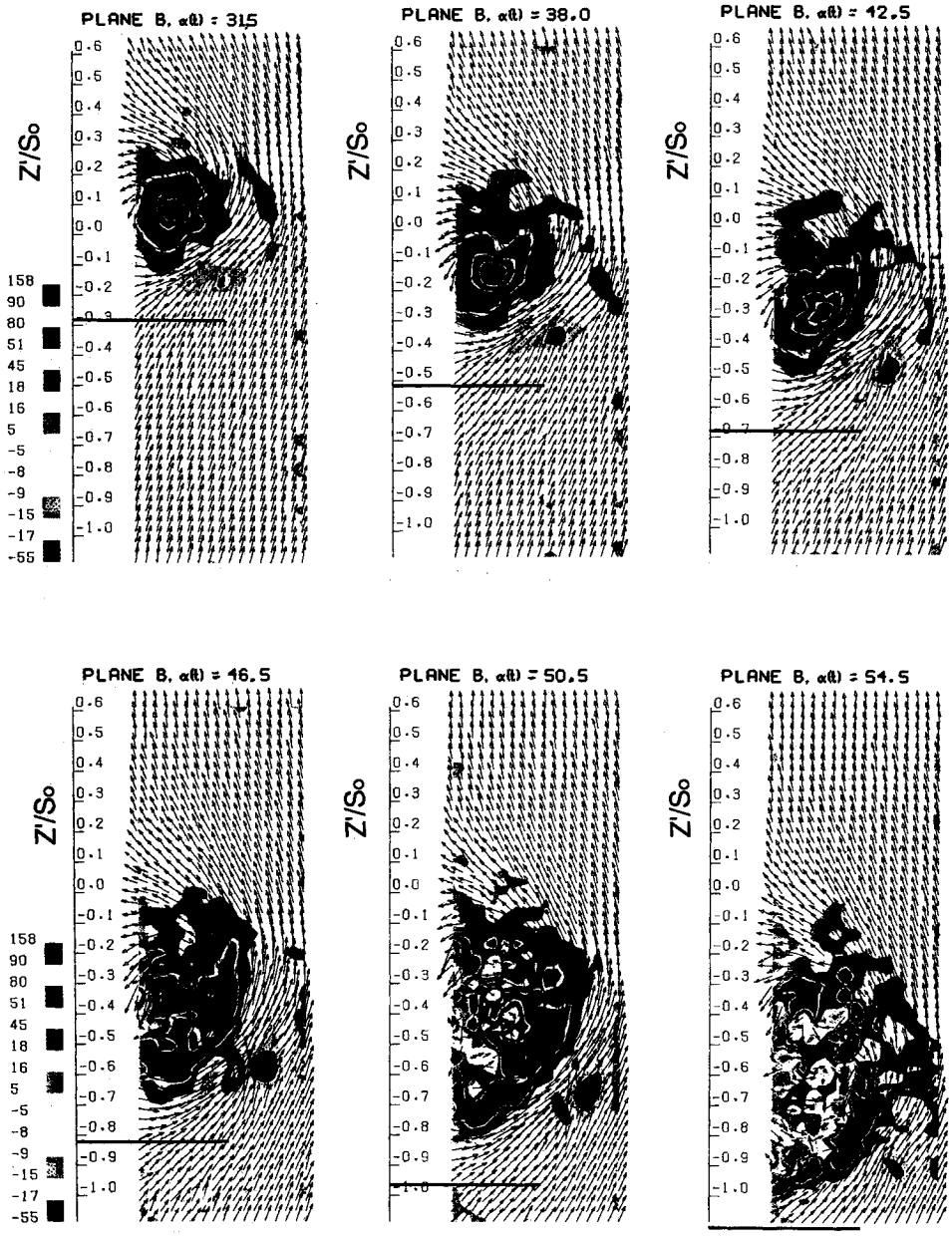


**Fig. 11 Development of vorticity and velocity field along plane B during pitch-up; all velocity measurements presented in this and subsequent plots have an estimated uncertainty of 2.5%.**

Evidence for the phenomenon of breakdown we can seek in terms of the rms of the pressure fluctuations as well. Once a vortex breaks down, the motion becomes unstable and the overall level of fluctuation increases. Earlier studies indicate that the rms of the pressure increases sharply beyond the location of breakdown. This is true for laminar as well as for turbulent flows. The rms of the pressure along the axial distance is plotted in Fig. 10. For angles of attack less than 48 deg, the levels of rms are uniformly low. At 48 deg though, the level indicates a moderate increase. For higher angles of attack, the rms increases further, but uniformly, along the entire chord of the wing. This confirms our earlier observation that breakdown emerges at about 46–48 deg and develops uniformly all along the chord, instead of creeping up from the trailing edge. The rms reaches its maximum at $\alpha = 58$ deg. With further increase of the angle of attack, the pressure fluctuations decrease. This implies that a dead-air region develops just like in the aft of any bluff body.

A sequence of frames representing cross sections of the flow along the plane B during pitch-up are displayed in Fig. 11. In these frames we plot the velocity vectors representing the projection of the local velocity on plane B. We also superimpose the component of vorticity normal to this plane, calculated by finite differences in terms of the velocity components,

$$\Omega_{X'} = \frac{C}{U}\left(\frac{\partial w}{\partial Y'} - \frac{\partial v}{\partial Z'}\right)$$

The narrow white bands between the shaded contours help distinguish between consecutive levels of vorticity. The vertical scale is measured along the axis $Z'$ in terms of half-spans $S_0$ (see Fig. 4). Distances in the horizontal direction are measured with the same scale. The thick horizontal line shown in these frames represents the projection of the trailing edge along the direction of the freestream on plane B. This provides an indication of the location of the wing.

Earlier studies[20,21] indicate that a seven-hole probe may interfere with the flow and actually induce vortex breakdown. In Ref. 29 it was demonstrated by comparing with LDV data that a seven-hole probe may actually induce breakdown if inserted in the core of the vortex but generates quite accurate data if positioned away from the core. This instrument can not be fully trusted to indicate when vortex breakdown occurs.

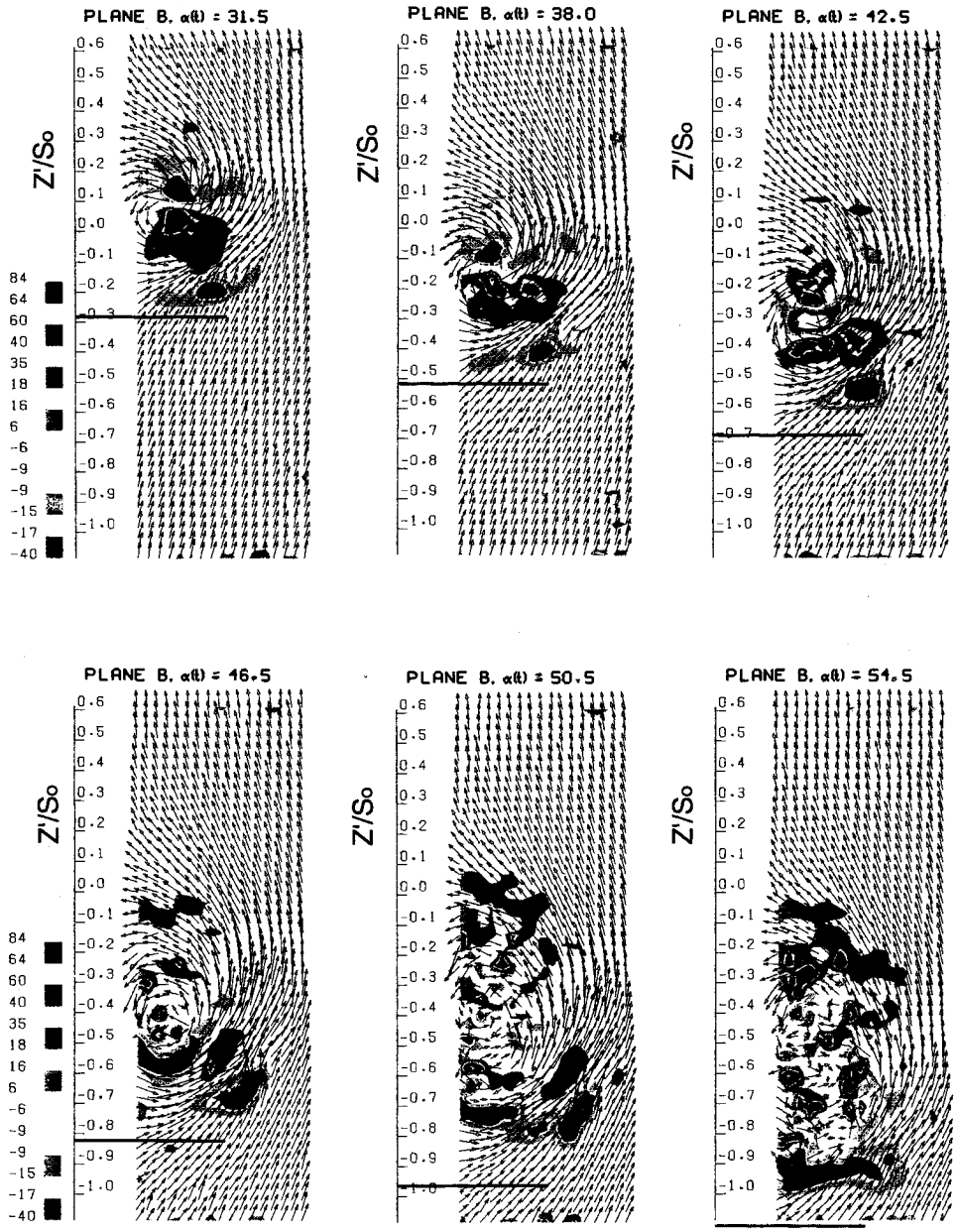


**Fig. 12 Development of the $Y$ component of vorticity superimposed on the velocity field in plane B.**

On the other hand, seven-hole probe readings are reliable, if they indicate a coherent vortex. When breakdown is detected with a seven-hole probe, one can conclude that this event would have occurred in undisturbed flow either at this angle of attack or at even higher angles of attack. The actual behavior can be obtained only by comparison with surface pressure distributions.

We observe that the magnitude of the vorticity in the core remains essentially constant until $\alpha = 46.5$ deg. Once again this is in agreement with our earlier observation with respect to pressure distributions. The vortex is pulled downward, following the motion of the wing. It starts at an elevation of about $Z'/S_0 = 0.2$ at $\alpha = 28$ deg and displaces to $Z'/S_0 = -0.3$ for $\alpha = 48$ deg. At higher angles of attack the vortex breaks down. Vorticity spreads out and reduces in magnitude. If we observe the velocity vectors for $\alpha = 50.5$ deg we notice that the core lacks any organization, but not far from the center of the vortex, the velocity distributions are coherent and the flow pattern is consistent with the vortical motion. This is one more piece of evidence confirming the fact that breakdown propagates from the core radially outward.

The negative vorticity present in all time frames up to an angle of attack $\alpha = 54.5$ deg, is not the secondary counter-rotating vortex that usually develops beneath the main leading-edge vortex. This negative vorticity is due to shedding of vorticity from the trailing edge. It should be observed that before breakdown occurs, the negative vortex follows the wing in its downward motion and also moves in the outboard direction, whereas the core of the leading-edge vortex maintains an almost constant spanwise location throughout the wing motion. Moreover, the negative vorticity region maintains its strength and organization even after the main leading-edge vortex has broken down.

In Fig. 12 we present frames of the $Y$ component of vorticity in plane B superimposed on in-plane velocity vectors. As expected, for a coherent vortex, the sign of the $Y$ component of vorticity changes from negative to positive as we move from the region above the vortex core to the one below it. This is an indication of the spiraling shape of the vorticity lines. In these frames, we have also captured the trailing-edge vortex (lower, negative-vorticity region) generated by the dynamic motion of the wing which forces the sharp trailing edge downward. This region persists, as it should, without a change of sign up to angles of attack as high as $\alpha = 58.5$ deg.

Figure 12 provides very interesting information on the relation between the circumferential component of vorticity and

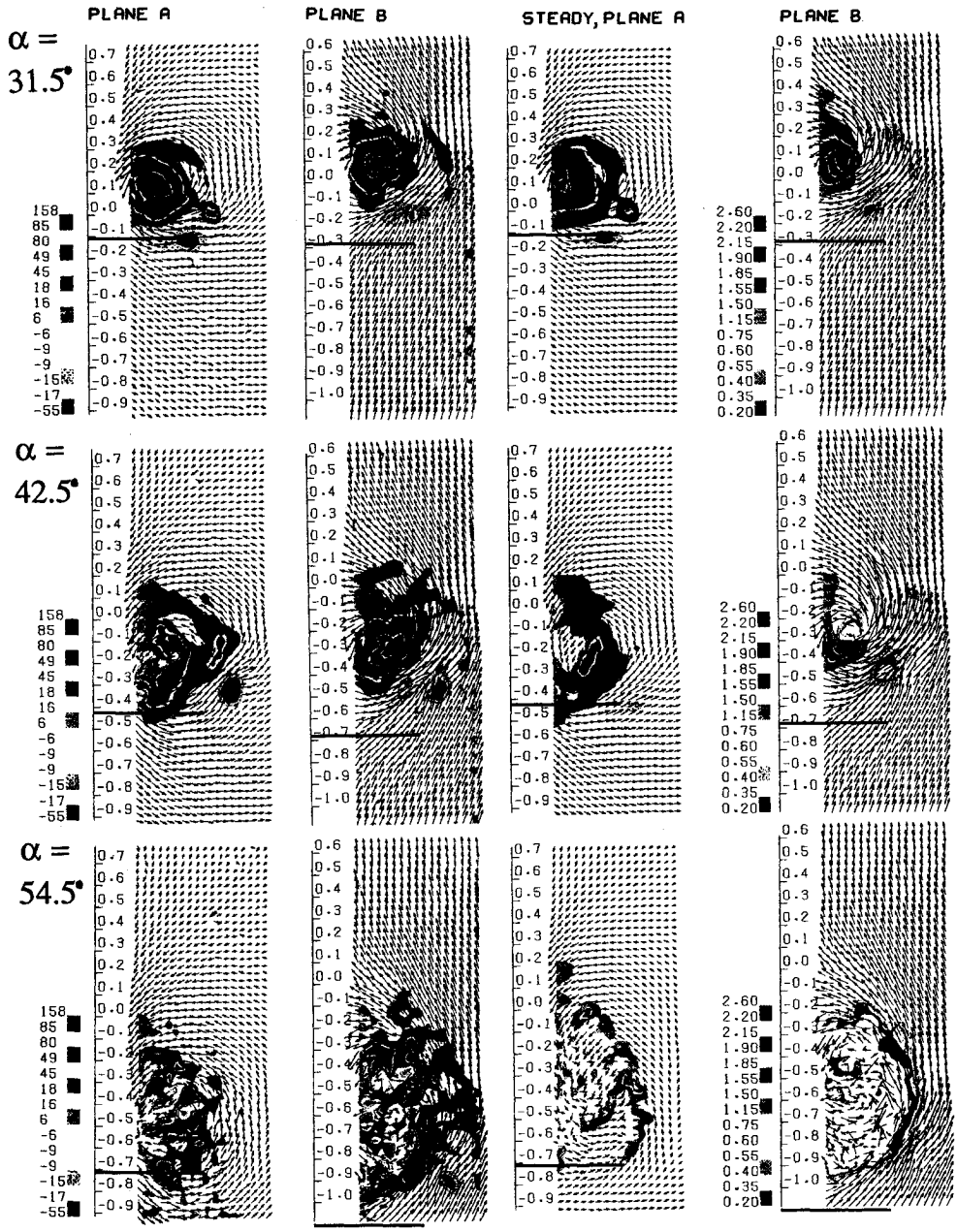


**Fig. 13 Flowfields in the wake of the model; column 1, vorticity and velocity in plane A during pitch-up; column 2, vorticity and velocity in plane B during pitch-up; column 3, vorticity and velocity for steady flow in plane A; column 4, axial component of velocity during pitch-up, in plane B.**

vortex breakdown. In the two frames, $\alpha = 31.5$ deg and $\alpha = 38$ deg, the circumferential vorticity component in the main vortex is positive (the counter-clockwise direction is defined as positive). This is obvious from the distribution of the $Y$ component of vorticity around the core: negative (or from right to left) above the core and positive below it. However, at $\alpha = 42.5$ deg the $Y$ component vorticity regions start rearranging themselves, and at $\alpha = 46.5$ deg, they have reversed their positions about the core: positive $Y$ component above the core and negative below it. This indicates a sign reversal of the circumferential vorticity component, from positive or counterclockwise to negative or clockwise. From the preceding it seems that this sign reversal of the circumferential vorticity component precedes breakdown as detected by axial vorticity. Both, circumferential vorticity and axial velocity breakdown, start exhibiting themselves at $\alpha = 42.5$ deg, whereas at this angle, the axial vorticity component is still coherent. The preceding observation should, in fact, be expected if one recalls Biot-Savart's law and how it relates the circumferential vorticity component to the axial velocity component: if the former has a positive sign, it induces a positive sign to the latter and vice-versa. In other words, positive circumferential vorticity accelerates the core axial velocity, but negative vorticity slows it down, until stagnation is achieved.

In Fig. 13 we present comparisons of velocity and vorticity fields along planes A and B for steady and unsteady cases. We also present the axial component of the velocity in terms of contours superimposed on the velocity vectors contained in the plane of measurement. It is very interesting to notice that in the fourth column of Fig. 13 and at $\alpha = 42.5$ deg a region of high and a region of low axial velocity coexist. Apparently, breakdown has just set in, propagating over the vortex cross section in an asymmetric fashion. It is possible that this asymmetry is caused by seven-hole probe intrusion effects. However, similar breakdown asymmetry in the steady case has been reported by Kegelman and Roos,[25] who used LDV measuring techniques. Of interest is also the fact that although the axial velocity starts exhibiting breakdown signs at $\alpha = 42.5$ deg, the axial vorticity, at the same angle, still seems unaffected. This phenomenon might be seen as evi-

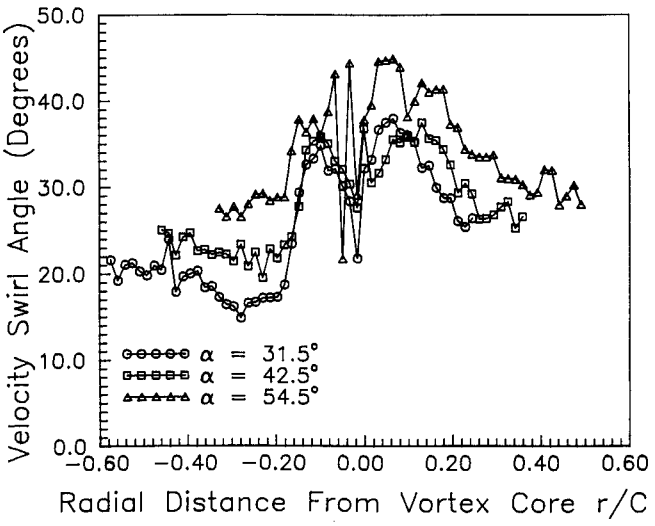


**Fig. 14 Helical angle of the velocity vector across the vortex.**

dence supporting recent theories which view breakdown as the last mechanism available to nature to transport and redistribute accumulated vorticity which can no more be convected downstream by the axial velocity. These observations and remarks indicate a cause-effect relationship between axial velocity breakdown and axial vorticity breakdown. If through some externally imposed mechanism, vorticity kept being transported downstream in sufficiently high rates, breakdown would never occur.

A comparison between the steady case and the unsteady case indicates significant differences in the core of the vortex. From Fig. 13, it is obvious that at $\alpha = 31.5$ deg the vortex is already broken down in the steady case (low axial vorticity magnitude in the core); whereas even at $\alpha = 54.5$ deg, the distributions in unsteady flow retain considerable levels of vorticity, axial velocity, in magnitude and coherence. The evidence provided here is in qualitative agreement with the flow visualization results presented in Refs. 4, 5, 7, 8, and 10 and carefully reviewed by Ashley et al.[33] Another interesting observation demonstrating the hysteresis effects between the unsteady case and the steady case is the following. At an angle of attack $\alpha = 31.5$ deg, where the wing is still in the very early stages of its pitch-up motion, the location of the trailing-edge vortex is the same for both cases, steady and unsteady. Note that the motion started from $\alpha = 28$ deg. Therefore, no significant hysteresis effects are expected yet. However, at an angle of attack $\alpha = 42.5$ deg, the locations of the trailing-edge vortex are significantly different. The vortex is located higher for unsteady flow than for steady flow. The foregoing observation, as expected, means that the vortex in the unsteady case does not have sufficient time to reach steady state and can not faithfully trace the motion of the trailing edge.

Finally, we present the helical angle of the streamlines. We define this quantity as the angle between the velocity vector and the axis of the vortex. In Fig. 14, we plot this quantity for three different values of the angle of attack, obtained during pitch-up. It appears that higher helical angles are found near the center of the vortex. Moreover, these angles increase as we move into breakdown. This fact implies that while the axial component of the velocity decreases as we enter breakdown, the swirling motion is sustained and thus larger helical angles are observed.

## IV. Conclusions

When a delta wing performs a dynamic ramp-like pitch-up maneuver, breakdown occurrence is greatly delayed, as many investigators have already pointed out. In this paper pressure and velocity data are presented to provide quantitative information on the breakdown process. For a 75-deg-sweep delta wing pitching up at a nondimensional pitch rate of 0.0089, breakdown does not cross the trailing edge before an angle of attack of 46 deg, although for the steady case this happens at about 32 deg.

Evidence is presented here that during dynamic pitch-up motions, breakdown does not creep up from downstream; but, instead, it appears almost simultaneously along the entire chord of the wing. It then spreads radially outward. Mean and rms pressure distributions as well as velocity field data were presented in support of this finding but more detailed data are necessary to confirm it. This is because even for steady flow, the location of breakdown moves up almost to the middle of the wing within an increase of 2 deg and then its upstream progression requires much larger changes of the angle of attack. Our data here capture the unsteady phenomenon every 2 deg of change in the angle of attack. Therefore, it is possible that breakdown propagates upstream with great speed instead of appearing simultaneously over the entire wing.

Detailed information is presented for the first time on the structure of the flow during the delay phase. The dynamic development of the flow lags behind the corresponding quasistate patterns. Our data indicate that the tip vortices retain a core with concentrated large values of vorticity and a strong axial velocity component for angles of attack as large as 46 deg. Breakdown follows and eventually a bluff body wake pattern sets in. Axial velocity breakdown seems to precede axial vorticity breakdown. The asymmetric structure of breakdown, observed in the steady case is exhibited in the dynamic case as well. It should be mentioned that the elevation of the vortex axis increases beyond $\alpha = 48$ deg and loss of pressure suction could be attributed to this fact as well. The amount of information here far exceeds the number of data included in our figures. We have stored the raw data for practically a continuous variation from $\alpha = 28$ deg to $\alpha = 64$ deg. These data are available to the readers of this journal. To obtain this information, please write directly to the last author.

## Acknowledgment

This work was supported by the Air Force Office of Scientific Research, Project AFOSR-91-0310 and was monitored by Daniel Fant.

## References

[1]Lambourne, N. C., Bryer, D. W., and Maybrey, J. F. M., "The Behavior of the Leading-Edge Vortices Over a Delta Wing Following a Sudden Change of Incidence," NPL Aero Rept. 1294-ARC 81 056, 1969.

[2]Gad-el-Hak, M., and Ho, C.-M., "Three-Dimensional Effects on a Pitching Lifting Surface," AIAA Paper 85-0041, Jan. 1985.

[3]Lee, M., Shih, C., and Ho, C.-M., "Response of a Delta Wing in Steady and Unsteady Flows," *Forum on Unsteady Flow Separation Proceedings*, Vol. 52, American Society of Mechanical Engineers A88-14141 03-34, New York, 1987, pp. 19–24.

[4]Naumowicz, T., Jarrah, M. A., and Margason, R. J., "Aerodynamic Investigation of Delta Wings with Large Pitch Amplitudes," AIAA Paper 88-4332, Aug. 1988.

[5]Brandon, J. M., and Shah, G. H., "Effect of Large Amplitude Motions on the Unsteady Aerodynamic Characteristics of Flat-Plate Wings," AIAA Paper 88-4331, Aug. 1988.

[6]Bragg, M. B., and Soltani, M. R., "An Experimental Study of the Effect of Asymmetrical Vortex Bursting on a Pitching Delta Wing," AIAA Paper 88-4334, Aug. 1988.

[7]LeMay, S. P., Batill, S. M., and Nelson, R. C., "Leading-Edge Vortex Dynamics on a Pitching Delta Wing," AIAA Paper 88-2559, Aug. 1988.

[8]Soltani, M. R., Bragg, M. B., and Brandon, J. M., "Experimental Measurements on an Oscillating 70-degree Delta Wing in Subsonic Flow," AIAA Paper 88-2576, Aug. 1988.

[9]Jarrah, M. A., "Low-Speed Wind-Tunnel Investigation of Flow about Delta Wings Oscillating in Pitch to Very High Angle of Attack," AIAA Paper 89-0295, Jan. 1989.

[10]Atta, R., and Rockwell, D., "Leading-Edge Vortices Due to Low Reynolds Number Flow Past a Pitching Delta Wing," *AIAA*

*Journal*, Vol. 28, No. 6, 1990, pp. 995–1004.

[11]Magness, C., Robinson, O., and Rockwell, D., "Control of Leading-Edge Vortices on a Delta Wing," NASA/AFOSR/ARO Workshop on Physics of Forced Separation, April 1990.

[12]Brandon, J. M., and Shah, G. H., "Unsteady Aerodynamic Characteristics of a Fighter Model Undergoing Large-Amplitude Pitching Motions at High Angles of Attack," AIAA Paper 90-0309, Jan. 1990.

[13]Thompson, S., Batill, S. M., and Nelson, R. C., "Delta Wing Surface Pressures for High Angle of Attack Maneuvers," AIAA Paper 90-2813, Aug. 1990.

[14]Magness, C., Robinson, O., and Rockwell, D., "Laser-Scanning Particle Image Velocimetry Applied to a Delta Wing in Transient Maneuver," *Experiments in Fluids* (to be published).

[15]Magness, C., Robinson, O., and Rockwell, D., "Unsteady Cross Flow on a Delta Wing Using Particle Image Velocimetry," *Journal of Aircraft*, Vol. 29, 1992, pp. 707–709.

[16]Herbst, W. B., "Dynamics of Air Combat," *Journal of Aircraft*, Vol. 20, No. 7, 1983.

[17]Hamilton, W. L., and Skow, A. M., "Operational Utility Survey, Supermaneuverability," Air Force Wright Aeronautical Labs., AFWAL-TR-85-3020, Sept. 1984.

[18]Nguyen, L. T., and Gilbert, W. P., "Impact of Emerging Technologies on Future Combat Aircraft Agility," AIAA Paper 90-1304, May 1990.

[19]Lee, M., and Ho, C.-H., "Lift Force of Delta Wings," *Applied Mechanics Reviews*," Vol. 43, May 1990, pp. 209–221.

[20]Taylor, S. L., Kjelgaard, S. O., Weston, R. P., Thomas, J. L., and Sellers, W. L. III, "Experimental and Computational Study of the Subsonic Flow about a 75° Swept Delta Wing," AIAA Paper 87-2425, May 1987.

[21]Meyers, J. F., and Hepner, T. E., "Measurement of Leading Edge Vortices from a Delta Wing Using a Three-Component Laser Velocimeter," AIAA Paper 88-2024, Jan. 1988.

[22]Payne, F. M., Ng, T. T., and Nelson, R. C., "Visualization and Wake Surveys of Vortical Flow over a Delta Wing," *AIAA Journal*, Vol. 26, No. 2, 1988, pp. 137–143.

[23]Kegelman, J. T., and Roos, F. W., "Effects of Leading-Edge Shape and Vortex Burst on the Flowfield of a 70-degree-Sweep Delta Wing," AIAA Paper 89-0086, Jan. 1989.

[24]Anders, K., "Measurement of Velocity Distribution in Delta Wing Vortices using Laser-Doppler Velocimetry," VKI PR 1981-03.

[25]Kegelman, J. T., and Roos, F. W., "The Flowfields of Bursting Vortices Over Moderately Swept Delta Wings," AIAA Paper 90-0599 Jan. 1990.

[26]Payne, F. M., Ng, T. T., and Nelson, R. C., "Seven-Hole Probe Measurement of Leading Edge Vortex Flows," *Experiments in Fluids*, Vol. 7, Jan. 1989, pp. 1–8.

[27]Pagan, D., and Solignac, J. L., "Experimental Study of the Breakdown of a Vortex Generated by a Delta Wing," *La Recherche Aerospatiale*, Vol. 3, No. 3, 1986, pp. 29–51.

[28]Nelson, R. C., and Visser, K. D., "Breaking Down the Delta Wing Vortex," AGARD Conference Proceedings, No. 494, July 1991.

[29]Rediniotis, O. K., Hoang, N. T., and Telionis, D. P., "Multi-Sensor Investigation of Delta Wing High-Alpha Aerodynamics," AIAA Paper 91-0735, Jan. 1991.

[30]Stewartson, K., and Hall, M. G., "The Inner Viscous Solution for the Core of a Leading-Edge Vortex," *Journal of Fluid Mechanics*, Vol. 15, 1965, pp. 306–338.

[31]Verhaagen, N. G., and Kruisbrink, A. C. H., "Entrainment Effect of a Leading-Edge Vortex," *AIAA Journal*, Vol. 25, No. 8, 1987, pp. 1025–1032.

[32]Rediniotis, O. K., "The Transient Development of Vortices Over a Delta Wing," Ph.D. Dissertation, Virginia Polytechnic Inst. and State Univ., Dept. of Engineering Science and Mechanics, Blacksburg, VA, Oct. 1992.

[33]Ashley, H., Katz, J., Jarrah, M. A., and Vaneck, T., "Survey of Research on Unsteady Aerodynamic Loading of Delta Wings," *Journal of Fluids and Structures*, Vol. 5, July 1991, pp. 363–390.